Eur. Phys. J. B **19**, 449–460 (2001)

THE EUROPEAN PHYSICAL JOURNAL B

EDP Sciences

Power injected in dissipative systems and the fluctuation theorem

S. Aumaître[1], S. Fauve[1,a], S. McNamara[2], and P. Poggi[3]

[1] Laboratoire de Physique Statistique[b], École Normale Supérieure, 24 rue Lhomond, 75005 Paris, France
[2] European Centre for Atomic and Molecular Computations, École Normale Supérieure de Lyon, 46 allée d'Italie, 69007 Lyon, France
[3] Dipartimento di Ingegneria Civile, University of Firenze, Via S. Marta 3, 50139 Firenze, Italy

Received 26 June 2000 and Received in final form 24 October 2000

Abstract. We consider three examples of dissipative dynamical systems involving many degrees of freedom, driven far from equilibrium by a constant or time dependent forcing. We study the statistical properties of the injected and dissipated power as well as the fluctuations of the total energy of these systems. The three systems under consideration are: a shell model of turbulence, a gas of hard spheres colliding inelastically and excited by a vibrating piston, and a Burridge-Knopoff spring-block model. Although they involve different types of forcing and dissipation, we show that the statistics of the injected power obey the "fluctuation theorem" demonstrated in the case of time reversible dissipative systems maintained at constant total energy, or in the case of some stochastic processes. Although this may be only a consequence of the theory of large deviations, this allows a possible definition of "temperature" for a dissipative system out of equilibrium. We consider how this "temperature" scales with the energy and the number of degrees of freedom in the different systems under consideration.

PACS. 05.40.-a Fluctuation phenomena, random processes, noise, and Brownian motion – 05.45.-a Nonlinear dynamics and nonlinear dynamical systems

1 Introduction

For most dissipative dynamical systems driven out of equilibrium by some forcing, the energy balance can be written in the form

$$\frac{\mathrm{d}E}{\mathrm{d}t} = P - D, \tag{1}$$

where $E(t)$ is the total energy of the system, constant in the absence of dissipative processes and external forcing, $P(t)$ is the power of the external forces that drive the system out of equilibrium, and $D(t)$ is the power lost by dissipative processes. Two types of problem, widely studied and for which equation (1) applies, are granular media and turbulent flows. Consider for instance a collection of macroscopic spherical particles enclosed in a vessel and excited by vibrating one boundary (see Fig. 6): then, E is the total kinetic energy of the particles, D is the power lost by inelastic collisions and P is the power injected into the granular medium by the motion of the boundaries (we neglect gravity). If a statistically stationary regime is reached, the temporal averages $\langle P\rangle$ and $\langle D\rangle$ are obviously equal

$$\langle P\rangle = \langle D\rangle \cdot \tag{2}$$

However, in any realistic experiment, the three quantities in (1), E, P and D, fluctuate in time, and one expects strong differences in their statistical behaviors. One has obviously

$$D(t) > 0, \tag{3}$$

whereas $P(t)$ takes negative values when a collision between a particle and the piston takes place when the piston is in descending motion. The same kind of remarks can be made on the example of turbulent flows. Consider an incompressible Newtonian fluid of density ρ and kinematic viscosity ν, driven by a volume force $\mathbf{f}(\mathbf{r},t)$. The equations of motion are

$$\nabla\cdot\mathbf{v} = 0, \tag{4a}$$

$$\rho\left[\frac{\partial\mathbf{v}}{\partial t} + (\mathbf{v}\cdot\nabla)\mathbf{v}\right] = -\nabla p + \rho\nu\Delta\mathbf{v} + \mathbf{f}, \tag{4b}$$

where $\mathbf{v}(\mathbf{r},t)$ is the velocity field and $p(\mathbf{r},t)$ is the pressure field. Multiplying (4b) with $\mathbf{v}(\mathbf{r},t)$ and integrating on the

[a] e-mail: fauve@physique.ens.fr
[b] UMR CNRS 8550

whole flow volume V gives equation (1) with

$$E = \frac{1}{2}\rho \int_V v^2 \mathrm{d}V, \tag{5a}$$

$$P = \int_V \mathbf{f}\cdot\mathbf{v}\,\mathrm{d}V, \tag{5b}$$

$$D = \rho\nu \int_V \omega^2 \mathrm{d}V, \tag{5c}$$

where $\boldsymbol{\omega}(\mathbf{r},t)$ is the vorticity field, $\boldsymbol{\omega} = \nabla\times\mathbf{v}$. We have assumed that the fluid is enclosed in a vessel of volume V and that the velocity vanishes at the boundaries.

We note that, as for the vibrated granular "gas", we have $D(t) > 0$ but $P(t)$ may take instantaneously negative values. This depends on the type of forcing of the flow (see the discussion below).

A problem of interest is the study of the statistical properties of the global quantities, E, P and D involved in equation (1). The term "global" should be understood as spatially integrated on the whole granular or fluid flow volume in the examples mentioned above, or on a surface if one considers the drag on a body in a turbulent flow or the heat flux in Rayleigh-Bénard convection. We have already studied the statistics of such global quantities [1–3] and emphasized that very little is known experimentally as well as theoretically about their fluctuation to mean ratio as the system is driven further and further in a turbulent regime. Our goal in the present study is to check a possible property of the probability density function (PDF) of the injected power, $P(t)$, known as the "fluctuation theorem". To the best of our knowledge, this property has been observed first for the PDF of the entropy production rate in a numerical simulation of a sheared fluid [4] and has been derived on a more mathematical basis for a particular class of time reversible dynamical systems [5].

Most dissipative dynamical systems are not time reversible, *i.e.* are not invariant under the transformation $t \to -t$. In references [4,5], the systems under consideration are made time reversible by choosing an appropriate form of dissipation for which equation (1) is transformed to

$$\frac{\mathrm{d}E}{\mathrm{d}t} = P - \alpha[\mathbf{X}(t)]D, \tag{6}$$

where $\alpha[\mathbf{X}]$ is a functional of the state $\mathbf{X}$ in the phase space of the system. The next step is to choose $\alpha[\mathbf{X}]$ such that a global quantity can be kept constant. For instance, if the total energy E is conserved, one has

$$P(t) = \alpha[\mathbf{X}(t)]D(t). \tag{7}$$

In the fluid example, this can be achieved by assuming that the kinematic viscosity is a functional of the velocity field, $\nu[\mathbf{v}]$. Note that $P(t) = \alpha[\mathbf{X}(t)]D(t)$ implies $\nu[-\mathbf{v}] = -\nu[\mathbf{v}]$ such that the transformed dissipation does not break $t \to -t$. References [4,5] have related $\alpha[\mathbf{X}]D$ to the fluctuations of the entropy production rate. Although the mean entropy production rate is positive, its instantaneous value may take negative values and the fluctuation theorem relates the probabilities of positive, respectively negative, production rates during a time interval τ. More precisely, writing

$$\epsilon_\tau(t) \equiv \frac{1}{\tau}\int_t^{t+\tau} P(t')\mathrm{d}t', \tag{8}$$

they have shown that the PDF Π obeys

$$\frac{\Pi(\epsilon_\tau = \epsilon)}{\Pi(\epsilon_\tau = -\epsilon)} \simeq \exp\,\beta\epsilon\tau \quad \text{for} \quad \tau\to\infty, \tag{9}$$

where β is a constant ($\tau\to\infty$ should be understood as τ large compared to the correlation time of $P(t)$).

For the dissipative systems we consider here, the instantaneous dissipation is positive but the injected power may change sign. Our goal is to check the possible validity of the relation (9) in the case of dynamical systems that are not made time reversible. We emphasize that the demonstration of the fluctuation theorem being intimately connected to time reversibility, it is not *a priori* obvious that this relation applies in the case of the dissipative dynamical systems considered here. However, we note that this relation has been shown in the case of the Langevin equation which is not a time reversible dynamical system [6].

This paper is organized as follows: we first consider in Section 2 a well-known shell model of turbulence and we show that the power injected into the system by the constant applied external force strongly fluctuates in time, sometimes taking negative values. We then study the probability density function of the injected power averaged over a time interval τ and show that equation (9) holds for this dissipative system. We repeat the same procedure in Section 3 for a granular gas of inelastically colliding particles agitated by vibrating one boundary of the container. In Section 4, we consider a Burridge-Knopoff spring-block model: a chain of blocks connected by springs, is pulled at one end with a constant velocity V on a rough surface (Fig. 9). We show again that the power of the pulling force strongly fluctuates and reaches negative values. Equation (9) holds for the granular gas as well as for the chain of blocks, but the constant β has a very different behavior in these two systems when the number of degrees of freedom is changed (the number of particles or the number of blocks). This is discussed in Section 5.

2 Power fluctuations in a shell-model of turbulence

2.1 The model

Shell models have been introduced as an attempt to mimic the dynamics of turbulence in Fourier space [7,8]. All the Fourier modes in the shell of wavenumbers k between $k_n = k_0\lambda^n$ and k_{n+1} (usually, and also in the present study, $\lambda = 2$) are represented by only one complex (or sometimes real) mode u_n, which is coupled to its nearest and next

nearest neighbours through quadratic interactions, such that the total energy

$$E = \frac{1}{2}\sum_{n=1}^{N} |u_n|^2, \tag{10}$$

is conserved in the absence of dissipation and forcing. The inviscid and unforced dynamics should also conserve the volume in phase space and possess the same scale invariance as the Euler equation. A class of shell models which has been introduced by Ohkitani and Yamada [9] and widely studied, is the following system of ordinary differential equations (GOY model):

$$\frac{\mathrm{d}u_n}{\mathrm{d}t} = \mathrm{i}k_n\left(u^*_{n+1}u^*_{n+2} - \frac{\alpha}{2}u^*_{n-1}u^*_{n+1} - \frac{1-\alpha}{4}u^*_{n-2}u^*_{n-1}\right) + f_n - \nu k_n^2 u_n \tag{11}$$

where the * stands for the complex conjugate, f_n is the Fourier complex amplitude of the force applied on the shell n, and ν is the kinematic viscosity. The parameter α determines the form of a second quadratic invariant of the inviscid and unforced system. The model with $\alpha = 1/2$ displays intermittency phenomena similar to the ones observed in fully developed three-dimensional turbulence [10,11]. We have made the conventional choices: $\lambda = 2$, $\alpha = 1/2$, $k_0 = 2^{-4}$, $f_n = f\,\delta_{n,4} = 5(1+\mathrm{i})\,10^{-3}\,\delta_{n,4}$, and we have varied ν in the range $10^{-9} < \nu < 10^{-4}$ with N chosen accordingly (see below).

Multiplying equation (11) by u^*_n and adding its complex conjugate, the summation on n leads to an equation of the form (1) with

$$P = \mathcal{R}(f\,u^*_4), \tag{12}$$

$$D = \nu\sum_{n=1}^{N} k_n^2|u_n|^2, \tag{13}$$

where $\mathcal{R}$ stands for the real part. As mentioned above, $D(t) > 0$, but the injected power, P, can take negative values depending on the phase of the Fourier component of the velocity at the wavenumber of the external forcing. If shell models are expected to mimic the properties that are believed to hold for turbulence, the mean injected (or dissipated) power should become independent of ν in the limit $\nu \to 0$. Surprisingly, this does not seem to have been precisely checked in the literature, probably because it is time consuming to perform an accurate check on a wide range of ν.

We have integrated (11) using the fourth order Runge-Kutta method with time step Δt, depending on the value of ν. As ν is decreased steeper gradients develop in a turbulent fluid, *i.e.* a larger number N of shells should be taken into account in the model. This can be understood easily from the form of the coefficient of the dissipative term, νk_n^2. The smaller is ν, the larger should be k_n in order to have a given amount of dissipation. The mean energy flux due to the nonlinear terms is constant through the shells of low k_n and equal to the mean energy dissipation rate $\langle D\rangle$, the dominant contribution of which corresponds to the large values of k_n. The transition wave number corresponds to the Kolmogorov scale, $k_\mathrm{d} = \langle D\rangle^{1/4}\,\nu^{-3/4}$, from which we can define n_d by $k_\mathrm{d} = k_0\lambda^{n_\mathrm{d}}$. The mean energy flux through each shell is constant almost up to the shell n_d. For each value of ν, we have taken the total number of shells, N, in order to have about 4 shells above n_d, *i.e.* in the dissipative range. We have also checked that increasing N does not modify the results. We thus have studied the following cases: $(\nu, N) = (10^{-4}, 15)$, $(10^{-5}, 17)$, $(10^{-6}, 20)$, $(10^{-7}, 22)$, $(10^{-9}, 29)$.

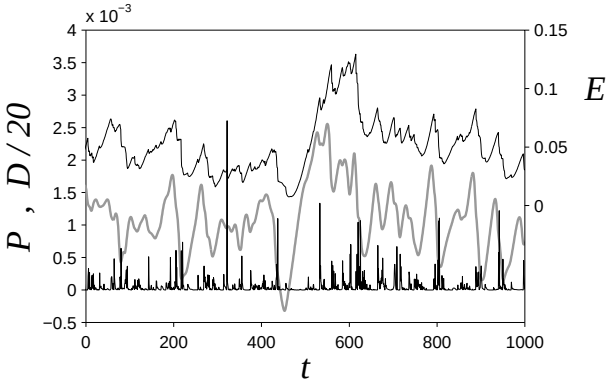

Fig. 1. Time recordings of the energy, E (upper curve), the injected power, P (thick grey curve) and the dissipated power, D (lower curve: $D/20$). $\nu = 10^{-6}$, $N = 20$.

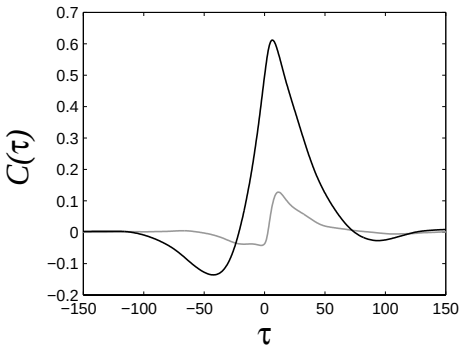

Fig. 2. Cross correlation function ($C(\tau) \equiv \langle (P(t) - \langle P\rangle)\,(E(t+\tau) - \langle E\rangle)\rangle / \sigma(P)\,\sigma(E)$) of the injected power and energy fluctuations showing a maximum larger than 0.6 for a time lag $\tau = 6.5$ (black curve). Cross correlation function of the injected power and the dissipation showing a smaller maximum for a time lag $\tau = 11.5$ (grey curve). $\nu = 10^{-7}$, $N = 22$.

Figure 1 displays a small sample of the direct recordings of the injected power, P, the energy, E, and the dissipated power, D, for $\nu = 10^{-6}$ and $N = 20$. The injected power displays strong fluctuations, almost 50% of the mean value, and can take negative values.

The characteristic correlation time is defined by the width at the value 0.5 of the autocorrelation function. We have $\tau_P \approx 15$ for $P(t)$ and $\tau_E \approx 34$ for $E(t)$ ($\nu = 10^{-7}$); they keep the same orders of magnitude for the whole

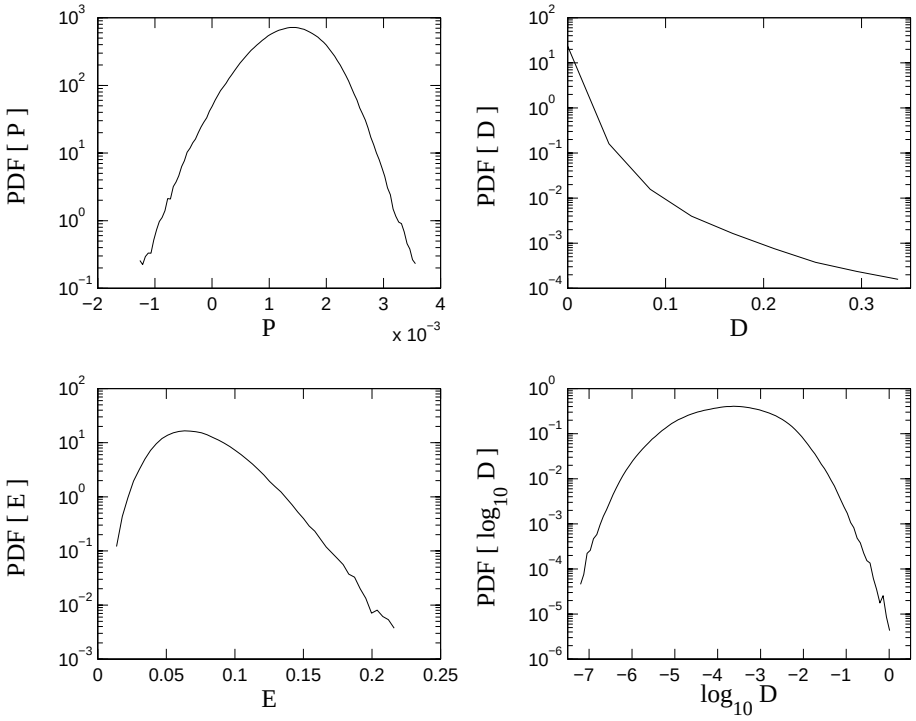

Fig. 3. Probability density function of the injected power, P, the energy, E, the dissipated power, D, and its logarithm. $\nu = 10^{-7}$, $N = 22$.

studied range of ν. The correlation time for $D(t)$ is much smaller and strongly depends on ν (0.025 for $\nu = 10^{-7}$).

The correlation between $P(t)$ and $E(t)$ is apparent in the time recordings of Figure 1. The cross-correlation of the injected power and the energy, displayed in Figure 2, is a more quantitative evaluation of this observation. It shows a maximum larger than 0.6 for a time lag $\tau = 6.5$. The cross-correlation of the injected power and the dissipation shows a smaller maximum for a time lag $\tau = 11.5$. Thus, dissipation bursts follow an increased energy which itself follows an additional amount of injected power.

The PDF of P, E, D and $\log D$ are shown in Figure 3 for $(\nu, N) = (10^{-7}, 22)$. As already observed, the injected power takes negative values. For $\nu = 10^{-7}$, we have 1.3% of negative events. The shape of the PDF of injected power is slightly asymmetric with a negative skewness. However, the skewness is positive for $\nu = 10^{-5}$ although the percentage of negative events is larger, 6.7%. The skewness vanishes for $\nu = 10^{-6}$. The probability of negative P values almost vanishes for $\nu = 10^{-4}$. The PDF of the energy is strongly asymmetric but this can be easily understood since the dominant contribution to E comes from the square of the modulus of u_n for small values of n. The very intermittent behavior of the dissipated power is apparent in the shape of its PDF, which roughly corresponds to a lognormal distribution, although its tails decay faster. The mean values of P and E together with their rms fluctuations are given in Table 1. Each numerical value is given with a number of digits consistent with the estimated error. Except for the case $\nu = 10^{-9}$, for which the integration time step is the shortest, the total integration time is longer that $10^5 \tau_P$.

As mentioned above, although $\langle P \rangle$ keeps the same order of magnitude when ν is varied from 10^{-4} to 10^{-9}, we do not find any clear tendency of an asymptotic regime $\langle P \rangle \to$ constant, when $\nu \to 0$. The rms fluctuations $\sigma(P)$ of the injected power related to the mean value, remain very large (roughly 50% as ν is decreased). Large fluctuations of $P(t)$ related to the mean value (roughly 10%) have been also observed in recent experiments on turbulent flows but they slowly decrease when the Reynolds number is increased [2,3,12]. The dissipated power is strongly intermittent and its characteristic time scale is much smaller than the one of the injected power. This behavior is not observed in numerical simulations of turbulent flows where the total dissipated power integrated on the whole flow volume, shows a characteristic timescale comparable to the one of the injected power [13]. In a turbulent flow, one may also argue that the relative width of the distribution of D should decrease when the viscosity is decreased, because the number of degrees of freedom is increased. The opposite behavior is observed in this shell model; the relative width of the distribution of D or $\log D$ increases significantly when ν is decreased. Let us thus note that, although shell models may display scaling exponents of the structure functions in qualitative agreement with real turbulence, they are in disagreement with elementary assumptions on turbulent flows such as the constant limit of the energy dissipation in the large Reynolds number limit.

Table 1. Mean values and standard deviations of the injected power, the dissipation and the energy in the shell model.

ν	10^{-4}	10^{-5}	10^{-6}	10^{-7}	10^{-9}
N	15	17	20	22	29
$\langle P\rangle$	1.491×10^{-3}	8.09×10^{-4}	1.014×10^{-3}	1.346×10^{-3}	1.0×10^{-3}
$\sigma(P)/\langle P\rangle$	0.358	0.678	0.530	0.417	0.57
$\langle D\rangle$	1.491×10^{-3}	8.09×10^{-4}	1.014×10^{-3}	1.346×10^{-3}	1.0×10^{-3}
$\sigma(D)/\langle D\rangle$	1.33	2.54	3.08	4.06	7.1
$\langle\log_{10} D\rangle$	-3.064	-3.606	-3.683	-3.730	-4.2
$\sigma(\log_{10} D)/\lvert\langle\log_{10} D\rangle\rvert$	0.1538	0.1953	0.2255	0.250	0.26
$\langle E\rangle$	0.0655	0.0565	0.0534	0.0724	0.062
$\sigma(E)/\langle E\rangle$	0.367	0.391	0.390	0.34	0.40

2.2 "Test of the fluctuation theorem"

The probability density functions of the injected power averaged over a time interval τ for $\tau = 15$, 30, 45, 60, are displayed in Figure 4 for the case $\nu = 10^{-7}$, $N = 22$, for which the correlation time is $\tau_P = 15$. As the averaging time is increased, the fluctuations decrease and the PDF shrinks around its mean value. The percentage of negative events thus decreases, which puts an upper limit on the value of τ for which the fluctuation theorem (Eq. (9)) can be checked on numerical or experimental data. When displayed as a function of the reduced variable $(\epsilon_\tau - \langle\epsilon_\tau\rangle)/\sigma_\tau$, where $\langle\epsilon_\tau\rangle$ is the mean value of ϵ_τ and σ_τ its standard deviation, all the PDFs roughly collapse on a Gaussian with zero mean and unit standard deviation. A closer inspection shows a slight departure from the Gaussian, which in this case, decreases as τ increases. Note however that as mentioned above, the shape of the PDF of P slightly depends on ν and is almost Gaussian for $\nu = 10^{-6}$; in that case, the shape of the PDFs of ϵ_τ deviates from a Gaussian as τ increases. This shows that $P(t)$ involves long-range correlations.

The quantity $\frac{1}{\tau}\log\frac{\Pi(\epsilon_\tau)}{\Pi(-\epsilon_\tau)}$, is plotted as a function of ϵ_τ in Figure 5 in order to check the fluctuation theorem. We observe that the form of equation (9) holds for any value of τ but that β depends on τ (as observed for reversible systems [4]). As τ increases, $\beta(\tau)$ tends to a constant value β in agreement with the fluctuation theorem (see the inset of Fig. 5). Without averaging on time, we have also checked that $\log\frac{\Pi(P)}{\Pi(-P)}$ is linear in P. One might then think that $\beta(\tau)$ could be represented over the entire range of τ as $\beta(\tau) = \beta(\tau=\infty) + \text{constant}/\tau$, as observed for temperature fluctuations in [30]; this is not true in our case: although $\beta(\tau)$ is linear in $1/\tau$ for large $1/\tau$, its difference from its asymptotic value β goes to zero much faster than $1/\tau$ for small $1/\tau$.

A similar analysis has been performed for $\nu = 10^{-6}$ and $\nu = 10^{-5}$. The case $\nu = 10^{-4}$ does not involve a large enough probability of negative values of P to allow a quantitative check of equation (9). We did not get enough statistics for the case $\nu = 10^{-9}$ because the number of required integration time steps is too large. The value of β is given in Table 2 as a function of ν. We note that βE divided by the number of shells in the inertial range is of order one, *i.e.* that $1/\beta$ scales like the mean kinetic energy per relevant degree of freedom.

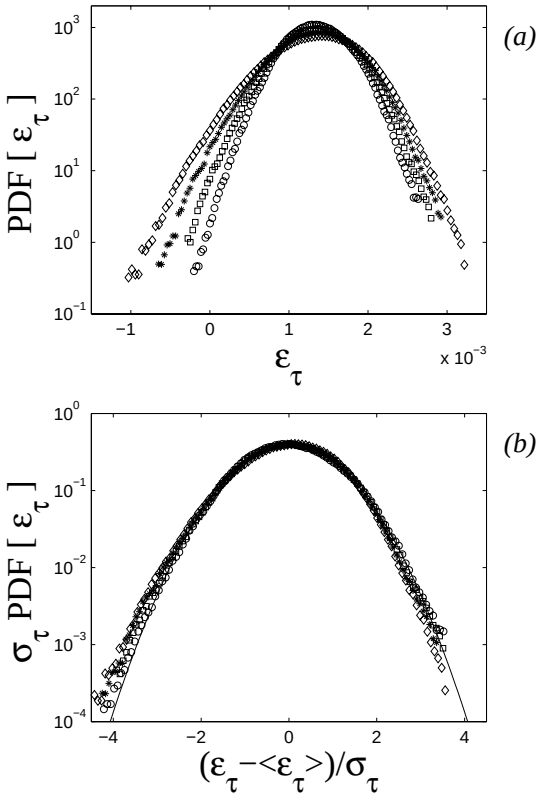

Fig. 4. (a) Probability density functions of the injected power averaged over a time interval τ: $\tau = 15$ ($\diamond$), $\tau = 30$ ($*$), $\tau = 45$ ($\square$), $\tau = 60$ ($\circ$). As the averaging time is increased, the fluctuations decrease and the PDF shrinks around its mean value. (b) When displayed as a function of the reduced variable $(\epsilon_\tau - \langle\epsilon_\tau\rangle)/\sigma_\tau$, all the PDFs roughly collapse on a Gaussian with zero mean and unit standard deviation (full line). A closer inspection shows a slight departure from the Gaussian, which in this case ($\nu = 10^{-7}$, $N = 22$), decreases as τ increases.

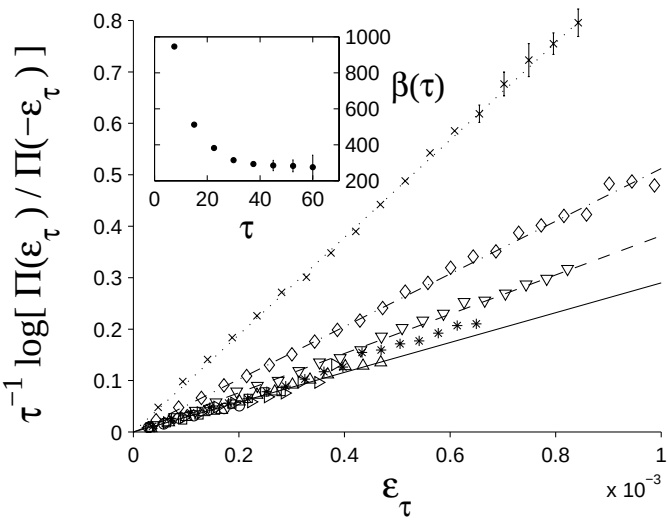

Fig. 5. The quantity $\frac{1}{\tau}\log\frac{\Pi(\epsilon_\tau)}{\Pi(-\epsilon_\tau)}$, is plotted as a function of ϵ_τ in order to check the fluctuation theorem: $\tau = 7.5(\times)$, $15(\diamond)$, $22.5(\bigtriangledown)$, $30(*)$, $37.5(\bigtriangleup)$, $45(\square)$, $52.5(\triangleright)$, $60(\circ)$. Straight line fits for $\tau = 7.5$ (dotted line), $\tau = 15$ (dashed-dotted line), $\tau = 22.5$ (dashed line), and for $30 \leq \tau \leq 60$ (full line), show that equation (9) holds with a value $\beta(\tau)$ shown in the inset, which tends to a constant when τ increases. $\nu = 10^{-7}$, $N = 22$.

Table 2. The value of β as a function of ν.

ν	10^{-5}	10^{-6}	10^{-7}
β	350	310	290
$\beta\langle E\rangle/(n_{\rm d}-3)$	1.8	1.2	1.3

3 Power fluctuations in a granular gas excited by vibrations

3.1 Energy flows in a granular gas excited by vibrations

Fluidization of a vibrated granular medium has been widely studied in the past years, both experimentally [14–16] and numerically [17]. Since a fraction $1 - r^2$ of the particle kinetic energy is dissipated during the collisions (r is the restitution coefficient, $0 < r < 1$), a stationary fluidized state necessitates a mean external flow of energy, $\langle P\rangle$, into the system. This is usually achieved by using a vibrating piston which compensates the mean dissipated energy flow $\langle D\rangle$ (see Fig. 6). These externally injected and dissipated energy flows have been studied numerically, but only their mean values have been considered so far, as well as the mean kinetic energy per particle, *i.e.* the "granular temperature".

We consider here the fluctuations of these quantities averaged over one period of vibration. The system is similar to the one studied in reference [17]. It consists of a two dimensional collection of inelastic hard disks of radius a, contained in a square container of length $L = 50\,a$. We take periodic boundary conditions along the x-axis and agitate the particles by moving the piston at period T

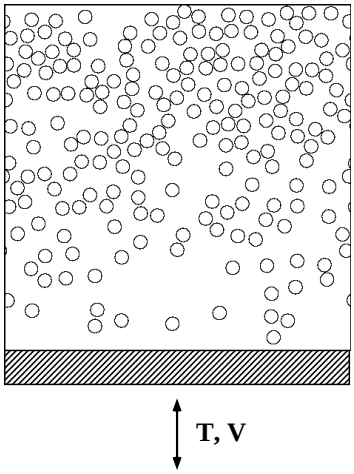

Fig. 6. A snapshot of the gas of inelastically colliding particles excited by vibrating horizontal boundaries. Periodic boundary conditions have been taken at vertical boundaries.

with a maximum velocity V; the periodic motion consists of an approximation of a sinusoidal wave by parabola. We take in all simulations: $T = 1$ and $V = 3$. We both consider the cases with and without gravity, g. For simplicity, the particle-wall collisions are assumed to be elastic. We use the standard event-driven method as in previous studies. We perform a simulation that records the values of $P(t)$ and $E(t)$ as well as the mean dissipation $D(t)$ averaged over one cycle, for each cycle of vibration. In our parameter range, there are at most a few collisions of particles with the vibrating piston during each cycle, and sometimes no collision. This explains the presence of the peak at zero value of P in the PDF of the injected power (see Fig. 7a). It displays an exponential tail of events with negative power for which there is a backflow of energy from the granular gas to the piston. The tail with events corresponding to a flow of energy into the gas is also roughly exponential. The precise shape of this PDF strongly depends on the parameter values of the model, in particular, on the restitution coefficient, r, the particle number, N, and on the value of the acceleration of gravity. Thus, there is no "universal" shape for the PDF of the injected energy, that obviously depends on the way the system is forced [20].

The mean values of the injected power, $\langle P\rangle$, and of the total kinetic energy, $\langle E\rangle$, together with their *rms* fluctuations, $\sigma(P)$ and $\sigma(E)$, are displayed in Table 3 as functions of the number of particles, N, and the restitution coefficient, r. First note that, contrary to fluid turbulence or to the shell model, the mean value of the injected power, $\langle P\rangle$, is not expected to saturate to a constant value as the coefficient governing dissipative processes, here $1 - r$, vanishes. We observe that when $r \to 1$, the particle mean velocity becomes larger and although the collisions are more elastic, the gas dissipates more energy. The mean injected power also increases correspondingly.

When gravity is added, it acts like an external field on the particles. Then we need to take into account the corresponding work in equation (1) or in other words, the

Table 3. Mean values and standard deviations of the injected power and energy for a granular gas with N particles of restitution coefficient r.

N	50	100	100 ($g = 0.2$)	200	200	200
r	0.9	0.9	0.9	0.9	0.95	0.99
$\langle P \rangle$	11.21	10.22	35.37	9.75	22.87	107.96
$\sigma(P)/\langle P \rangle$	1.50	1.40	0.85	1.37	0.98	0.67
$\langle E \rangle$	287.46	194.32	412.59	136.63	372.28	2970
$\sigma(E)/\langle E \rangle$	0.17	0.17	0.11	0.19	0.13	0.079

amount of potential energy converted into kinetic energy E. Thus, the total weight of the particles times the vertical velocity of the center of mass should be added to the part of P due to the collisions with the piston. The third column of Table 3 shows that gravity increases the mean value of E and P but decreases the relative fluctuations.

The PDF of the total kinetic energy E and of the dissipation D are smoother than the one of the injected power, although strongly asymmetric toward large values of the energy and the dissipation (Fig. 7b, c). It is tempting to fit these PDF using the gamma distribution of the form $x^{\frac{n}{2}-1} \exp -\alpha x$, also known as the "chi-square" distribution [18]. Indeed, it is known that the sum of the squares of mutually independent normal variables has a PDF of this form, a well known example being the kinetic energy of a perfect gas [18]. n is the number of variables in the sum and is called the number of degrees of freedom of this distribution.

In a regime without clustering, the PDF of E is reasonably fitted by the gamma distribution but with n smaller than $2N$ (in 2 space dimensions) which shows that the number of effective degrees of freedom is decreased because of the inelasticity of the collisions.

The PDF of D is also reasonably fitted by the gamma distribution in a regime without clustering. One observes that n increases when $r \to 1$ or when N is increased. However, for r fixed, the increase of n is not linear in N and seems to saturate when N is increased. In the studied range of parameters, n is smaller than the number of collisions per vibration cycle.

We expect the gamma distribution to be only an approximation of the PDF of E or D because the added random variables are no longer independent normal variables when the collisions are inelastic. However, the dependence of n on the system parameters (r, N, ...) may be interesting to study further in order to get insights in the behavior of a granular gas.

3.2 "Test of the fluctuation theorem"

The quantity $\frac{1}{\tau} \log \frac{\Pi(\epsilon_\tau)}{\Pi(-\epsilon_\tau)}$, is plotted as a function of ϵ_τ in Figure 8 in order to check the fluctuation theorem. We have not considered the values of ϵ_τ close to zero because of the large error bars due to the peak of events with zero injected power in Figure 7a. We observe that equation (9) holds for any value of τ. Moreover, contrary to the shell model, here $\beta(\tau)$ does not depend on τ. We observe in Figure 8 that $\frac{1}{T} \log \frac{\Pi(P)}{\Pi(-P)}$ displays roughly the same slope β as a function of the injected power P. This is probably related to the fact that the injected power during one vibration cycle is not correlated with the one during the previous cycle.

Table 4. The value of β as a function of r and N.

N	50	100	100 ($g = 0.2$)	200	200	200
r	0.9	0.9	0.9	0.9	0.95	0.99
$\frac{\beta\langle E \rangle}{N}$	1.10	0.42	0.6	0.34	0.45	0.75

The value of β is given in Table 4 as a function of the number of particles N and their restitution coefficient r. We note that $\beta\langle E \rangle/N$ is of order one and that it is decreased either by decreasing the restitution coefficient, r, or by increasing the number of particles, N. This dependence is consistent with previous studies [19], that show that the granular gas exhibits stronger and stronger correlations and clustering when either N or $(1-r)$ increases at fixed volume. This suggests that the decrease of $\beta\langle E \rangle/N$ when r is decreased for $N = 200$, is related to the fact that the effective number of degrees of freedom of the system decreases. Note also that there is no clear behavior of $\beta\langle E \rangle$ as a function of N for $r = 0.9$. However, it should be emphasized that we have obtained the same value for β when the particle number is multiplied by 2 at fixed density ($N = 100$, $L^2 = 2500a^2$ and $N = 200$, $L^2 = 5000a^2$) (see the discussion below).

4 Power fluctuations in a spring-block model

4.1 The model

We consider a chain of blocks connected by linear springs and pulled at one end with a constant velocity V (Fig. 9). The blocks are on a rough surface and, as time evolves, a given block slips if the elastic force applied to it by the connecting springs exceeds the static friction force. This model, as well as another one where each block is also directly connected to the driving device, have been proposed by Burridge and Knopoff to model earthquakes [21]. It has been shown that when the dynamic friction force is a decreasing function the the block velocity, these models display random slipping events that involve n blocks

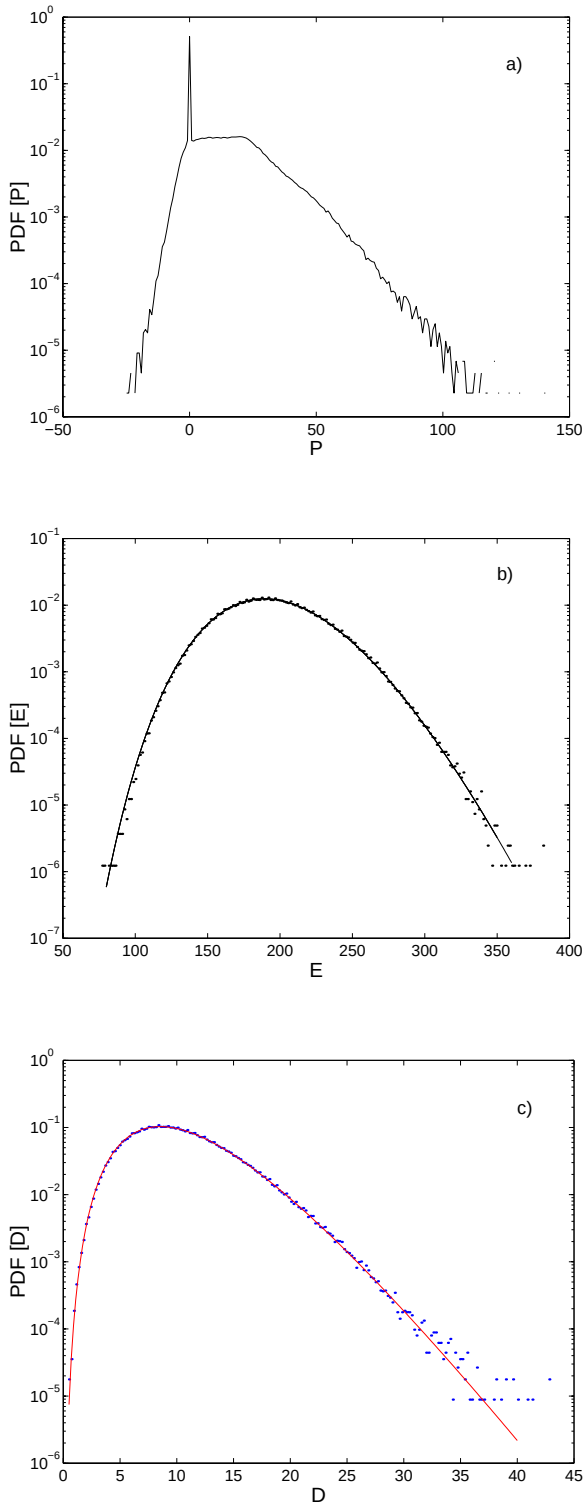

Fig. 7. (a) Probability density function of the injected power, P ($N = 200$, $r = 0.9$). The peak at zero corresponds to the cycles of vibration which involve no collision of a particle with the vibrating boundaries. (b) Probability density function of the kinetic energy E of the particles and its fit with a gamma distribution (full line). (c) Probability density function of the dissipated power and its fit with a gamma distribution (full line).

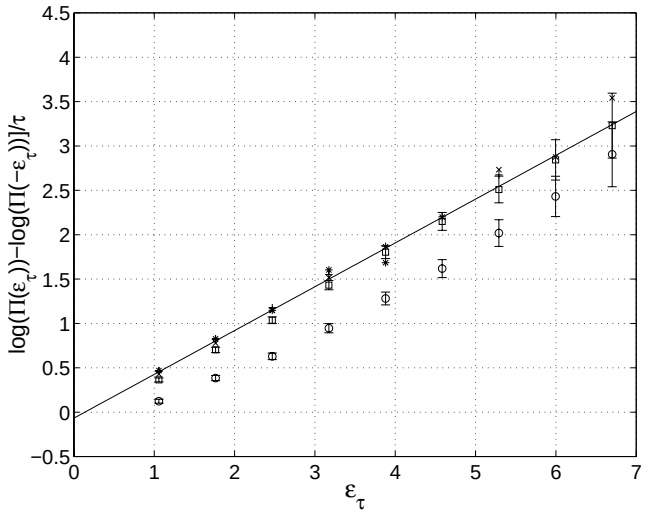

Fig. 8. The quantity $\frac{1}{\tau}\log\frac{\Pi(\epsilon_\tau)}{\Pi(-\epsilon_\tau)}$, is plotted as a function of ϵ_τ in order to check the fluctuation theorem. $\tau = 2T(\square)$, $3T(\times)$, $4T(+)$, $5T(*)$. Straight line fit (full line). Note that in this example β does not depend on τ and that the injected power itself displays roughly the same slope β ($\circ$).

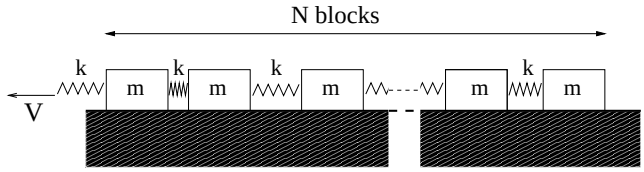

Fig. 9. Sketch of the Burridge-Knopoff model: N blocks of mass m, connected with springs of constant stiffness k, are pulled on a rough plane at constant velocity V.

($1 \leq n \leq N$, where N is the total number of blocks of the chain) [22,23]. The main motivation was to study the scaling properties of the probability distribution function of n in order to get insights in the scaling properties of earthquake magnitudes. We consider here the model studied in [23] but with different motivations. Our aim is to study the temporal dynamics and statistics of global quantities, such that the length of the chain $L(t)$, the power dissipated by the friction force, $D(t)$, or the one injected into the system by the operator pulling at constant velocity, $P(t)$. Our first motivation is to study how the fluctuations of these "macroscopic" quantities relative to their mean value, behave as the number of degrees of freedom, *i.e.* here the number of blocks, N, is increased. Is the ratio of fluctuation size to the mean value reduced when N is increased, and if yes what is the corresponding law? Our second motivation is to study the statistical properties of the injected power, $P(t)$. When the blocks are at rest, the operator's work is positive and increases the elastic potential energy of the system. During a slipping event, one part of the elastic energy is dissipated by the friction force but another part may be given back to the operator, *i.e.* $P(t) < 0$. Of course, on average, $\langle P\rangle = \langle D\rangle > 0$. We study the events with negative $P(t)$ and check the prediction of the "fluctuation theorem".

We use notation similar to that of reference [23]. Defining the rescaled displacement of the jth block, $U_j = kX_j/F_o$, where F_0 is the static friction force and k is the spring constant, we get the non-dimensional equations of motion

$$\begin{cases} \ddot{U}_i = (U_{i+1} - 2U_i + U_{i-1}) - \frac{1}{1+2\alpha\dot{U}_i} & \text{if } \dot{U}_i > 0, \\ \dot{U}_i = 0 & \text{if not.} \end{cases} \quad (14)$$

Time is rescaled using the characteristic spring frequency $\sqrt{k/m}$. The second term in the right hand side of equation (14) is the dynamic friction force; it should decrease with the velocity in order to get erratic sliding motions of the blocks. α characterizes the dependence of the friction force on the block velocity. Contrary to reference [23], the Nth block is not kept at a fixed position but moves freely. The boundary conditions are thus: $U_0 = V\sqrt{mk}\,t/F_0$ and $U_{N+1} = U_N$.

4.2 Macroscopic parameters and their fluctuations in the limit of large number of blocks

We multiply equation (14) by U_i and sum over all blocks. We find

$$P(t) = \frac{V}{V_0}(U_0(t) - U_1(t)) \quad (15a)$$

$$D(t) = \sum_{i=1}^{N} \frac{\dot{U}_i(t)}{1 + 2\alpha\dot{U}_i(t)} \quad (15b)$$

$$E(t) = \frac{1}{2}\left[\sum_{i=1}^{N} \dot{U}_i(t)^2 + \sum_{i=0}^{N} (U_{i+1}(t) - U_i(t))^2\right] \quad (15c)$$

where V_0 is the characteristic speed $F_o/\sqrt{mk}$. Figure 10 shows the PDFs of P, E, D and the one of the extension of the chain length $L(t) = U_1(t) - U_N(t)$, for $N = 200$ with a dimensionless pulling velocity equal to 0.1 and $\alpha = 0.5$. We first notice that none of these quantities displays Gaussian fluctuations. The skewness of the injected power is negative (equal to -0.65) as well as the one of the length extension (equal to -0.71) whereas the one of the energy is strongly positive (equal to 1.55). The injected power displays 10 to 20% of negative events. The dissipated power D is always positive as expected from (15b) since $\dot{U}_i > 0$. Its most probable value is zero, *i.e.* corresponds to blocks at rest, and its PDF presents a power-law fall-off. Note also that the pulled chain is extended on average since $\langle L\rangle > 0$. The PDFs of all these quantities keep the same form when the number of blocks increases from 20 to 2000.

It is particularly interesting to consider the mean value and the ratio of the fluctuations to the mean, for these four "macroscopic" quantities, as the number of blocks increases. This is shown in Table 5. First, none of the averaged quantities grows linearly with the number of blocks as would be expected if some thermodynamic limit were reached. The mean energy and the mean extension length grow faster whereas the mean injected power grows slower. We have respectively $\langle E\rangle \propto N^{2.23}$, $\langle L\rangle \propto N^{1.6}$ and $\langle P\rangle = \langle D\rangle \propto N^{0.5}$. Moreover the relative fluctuations which are very large (about 80% for the energy and up to more than 100% for the injected power), do not decrease when N is increased. The relative fluctuations of the injected and dissipated power even increase. These facts result from a long-range correlation between blocks. Indeed, if the spatial correlation function, $\langle U_n(t)U_{n+p}(t)\rangle$, is averaged over a sufficiently long time, it does not vanish when p increases. Despite their erratic motions, the blocks are strongly correlated in the chain. This will be also apparent in the dependence of β *versus* N in equation (9).

4.3 "Test of the fluctuation theorem"

It is easy to check the fluctuation theorem on this system because of the rather large percentage of negative events in the injected power. The quantity $\frac{1}{\tau}\log\frac{\Pi(\epsilon_\tau)}{\Pi(-\epsilon_\tau)}$, is plotted as a function of ϵ_τ in Figure 11. We observe that equation (9) holds for large values of τ and that $\beta(\tau)$ converges to a constant for τ larger than $10\,t_c$ where t_c is the correlation time of $P(t)$. Slight departures from linearity are observed for small values of τ.

The value of β is given in Table 6 as a function of the number of blocks N. Contrary to the two previous examples, $1/\beta$ scales like the mean energy and not the mean energy divided by the number of blocks (see below). This is in agreement with the fact that the blocks are strongly correlated whatever the length of the chain.

5 Discussion and concluding remarks

5.1 The theory of large deviations and the form of equation (9)

The demonstration of the fluctuation theorem being connected to time reversibility, it may be *a priori* surprising that the three different dissipative systems we considered here follow relation (9) so nicely. The observation of a law of the form (9) should thus have a deeper basis and not be restricted to reversible Anosov systems. It has been pointed out that the fluctuation theorem is "a large deviation theorem" [5,24]. Indeed, ϵ_τ being the average of the injected power on a time interval τ, we have for the probability density $\Pi(\epsilon_\tau = \epsilon)$

$$\Pi(\epsilon_\tau = \epsilon) \propto \exp \tau f(\epsilon) \quad \text{for} \quad \tau \to \infty, \quad (16)$$

according to the theory of large deviations [25,26]. In the systems investigated here, $\langle P\rangle = \langle D\rangle$ has a positive finite value. Thus, the probability of observing values of ϵ_τ close to zero is very small as soon as τ is large compared to the correlation time of $P(t)$, and the leading order Taylor expansion of (16) around $\epsilon = 0$ gives (9) with $\beta = 2\,f'(0)$. This may be the very simple reason for which a law of the form (9) is observed for all the dissipative systems considered here. In the case of reversible systems, it has been shown that the quantity $\frac{1}{\tau}\log\frac{\Pi(\epsilon_\tau)}{\Pi(-\epsilon_\tau)}$ is linear in ϵ [4,5].

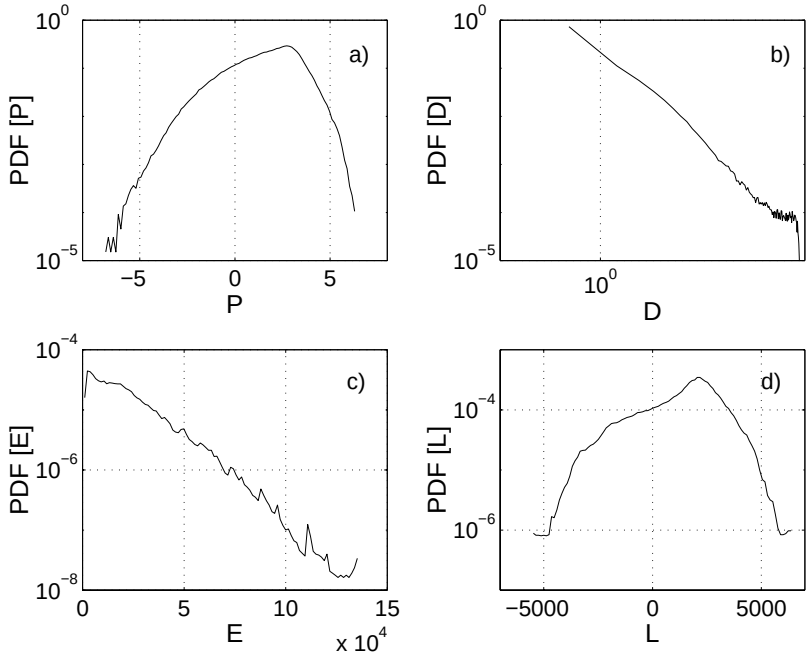

Fig. 10. Probability density function of the injected power, P, the total energy, E, the dissipated power, D, and the length extension of the chain, L, $\alpha = 1$, $V = 0.1$, $N = 100$.

Table 5. Mean values and standard deviations of the energy, the length extension, the injected power, and the dissipation for the spring-block model.

N	20	50	100	200	500	1000
$\langle E\rangle$	118.53	889.8	4267.5	2.02×10^4	1.67×10^5	7.014×10^5
$\sigma(E)/\langle E\rangle$	0.79	0.77	0.79	0.80	0.80	0.82
$\langle L\rangle$	33.31	152.9	459.1	1347.6	6008.1	1.737×10^4
$\sigma(L)/\langle L\rangle$	1.13	1.11	1.20	1.29	1.36	1.32
$\langle P\rangle$	0.491	0.822	1.158	1.639	2.506	3.539
$\sigma(P)/\langle P\rangle$	0.67	0.77	0.90	1.00	1.18	1.24
$\langle D\rangle$	0.492	0.824	1.159	1.642	2.500	3.544
$\sigma(D)/\langle D\rangle$	2.18	2, 60	3.01	3.41	4.15	4.69

Although this property is also observed in our simulations, we cannot claim that higher powers of ϵ are absent; they may just be too small to be observed.

It should be noted also that a law of the form (9) is observed for small values of τ and even for $P(t)$ itself, in the examples of the shell model and the granular gas. We may explain this behavior by using the large deviation theorem for $P(t)$ considered as an average on the whole system. Then β should be linear in N, the number of degrees of freedom of the system, as it is observed. Note that since $P(t)$ takes negative values with a larger absolute value than ϵ_τ, one may expect that nonlinear terms in ϵ, if they exist, would be more easily probed. This is not the case for the shell model since all PDFs are roughly Gaussian (see Fig. 4b) which implies that a law of the form (9) should be observed anyway. In the case of the granular gas, the PDF of $P(t)$ is very far from Gaussian. With the parameters of Figure 7a, it has an exponential tail on the range $P < 0$ and is roughly constant on the symmetric interval range $P > 0$ (in one excludes the peak for $P = 0$). Thus, one observes that (9) should hold on the interval range on which $\Pi(P)$ and $\Pi(-P)$ can be compared. However, we cannot exclude that longer statistics involving more negative values of P, do not show a difference from (9).

The main interest of (9) is that, β being homogeneous to the inverse of an energy, it could be used to define a "temperature" for a dissipative system out of equilibrium. We have thus considered how β^{-1} scales with the mean energy $\langle E\rangle$ and the number of degrees of freedom of the systems we have studied. The example of the granular gas is instructive. In the case of elastic collisions one expects $\beta\langle E\rangle/N = 1$ from the equipartition of energy. We observe in Table 4 that $\beta\langle E\rangle/N$ is indeed of order one and that it decreases when the particle number N is increased or when the restitution coefficient r is decreased. One also observes that $\beta\langle E\rangle/N$ is only slightly modified when an external gravity field is added. More importantly, in the parameter range of our studies (*i.e.* without clustering),

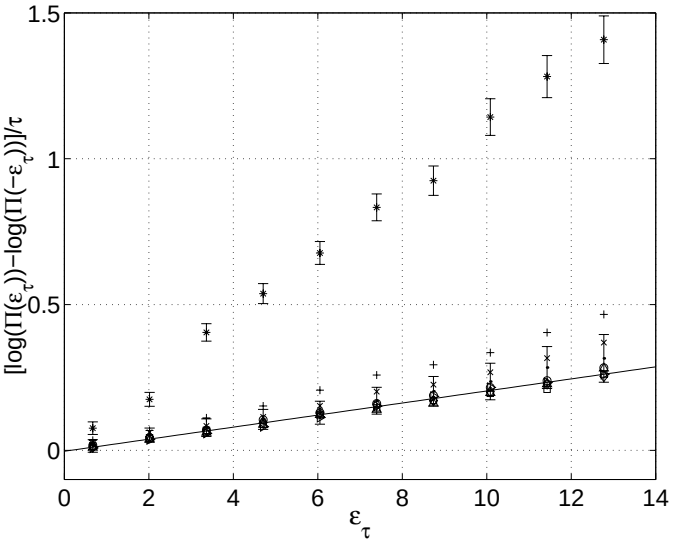

Fig. 11. The quantity $\frac{1}{\tau}\log\frac{\Pi(\epsilon_\tau)}{\Pi(-\epsilon_\tau)}$, is plotted as a function of ϵ_τ in order to check the fluctuation theorem: $\tau = t_c(*)$, $4t_c(+)$, $6t_c(\times)$, $8t_c(\bullet)$, $10t_c(\circ)$, $12t_c(\diamond)$, $14t_c$ $(\square)$, $16t_c$ $(\triangle)$, $20t_c(\triangleright)$. Straight line fit for $\tau > 10t_c$ (full line). $\alpha = 0.5$, $V = 0.1$, $N = 200$.

β is unchanged when the particle number is doubled at fixed density. Using β^{-1} as a definition of "temperature" in this system looks rather reasonable from these qualitative considerations. The situation is similar in the shell model where $\beta\langle E\rangle$ is roughly proportional to the number $n_d - 3$ of shells in the inertial range when the viscosity is varied (see Tab. 2). Note however that these two dissipative systems have a qualitatively different zero dissipation limit. In the case of the shell model, the mean injected or dissipated powers keep the same order of magnitude when ν decreases whereas in the granular gas, they strongly increase when $r \to 1$, but in both cases β^{-1} scales like the mean energy per degree of freedom. The situation is different in the spring-block example where $\beta\langle E\rangle$ is almost unchanged when the number of blocks is increased from 20 to 1000. As we already noticed, this system involves strong long-range spatial correlations among the blocks. Thus, increasing the number of blocks does not lead to an increase of the number of the relevant degrees of freedom of the system. It is satisfactory that this peculiar behavior of the system is apparent in the behavior of β as a function of N. Thus, trying to extend the concepts introduced in the fluctuation theorem to dissipative (non time reversible) dynamical systems, leads to a possible definition of a "temperature" which characterizes rather well some qualitative features of these systems.

5.2 Experimental checks of the fluctuation theorem

The next step is of course to ask whether these concepts could be of some use in real experiments, for instance in turbulence, for which it has been already proposed to use the fluctuation theorem [28]. The problem we have to deal with in the case of most experiments on turbulent flows is

Table 6. The value of β as a function of N.

N	20	50	100	200	500	1000
$\beta\langle E\rangle$	3.93	3.74	2.94	2.83	2.92	3.33

that $P(t)$ stays positive. If the flow is generated by a constant volume force (the gravity field for instance), equation (5b) shows that it is very unlikely that $P(t)$ takes negative values (which would correspond to a complete reversal of the mean flow). With a spatially periodic forcing, $P(t)$ is proportional to a Fourier component of the velocity field at the forcing wavenumber, and takes negative values if the instantaneous velocity field and the forcing are out of phase. With a sinusoidal forcing in time, $P(t)$ takes negative values if the forcing frequency is smaller or comparable to the one of the large scales of the flow. Thus, it seems that the possible use of the "fluctuation theorem" may depend on the way the flow is forced, which is a rather negative aspect for a general law.

In the case of flows with $P(t) > 0$, a possibility would be to consider the power injected in a finite subset of the flow. If its volume is taken small enough, the injected power is more likely to take negative values. However, this would lead to rather difficult measurements involving the evaluation of surface terms. A Lagrangian measurement, *i.e.* the power injected in a small volume of fluid particles advected by the flow, is even more out of reach. Thus, attempts of demonstrating a local version of the fluctuation theorem [27], although interesting and far from being an obvious extension of (9) [29], are likely to be of little use for the interpretation of experimental results.

It is of course possible to try to check (9) with any local field measured in a turbulent flow. This has been performed with local temperature fluctuations in Rayleigh-Bénard convection [30]. Although more than vaguely related to the injected power or to the entropy creation rate, it has been shown that the local temperature fluctuations follow a law of the form (9). The locally measured temperature fluctuations have zero mean in the horizontal mid-plane (contrary to the heat-flux) and the appropriate choice of the vertical position of the temperature probe in fact arbitrarily defines a zero temperature in the temperature fluctuations PDF. One may follow the same procedure for any random signal. Taking the pressure field in a turbulent flow for instance, we have arbitrarily defined a zero pressure, and observed that, provided it does not correspond to the mean pressure, a law of the form (9) is observed [31]. Of course, the value of τ required for convergence to (9) depends on the choice of the origin as well as the value of β. This is obviously related to the law of large deviations, and possible cubic or higher order terms in ϵ are not probed probably because they are too small.

It is only when a power is measured (or a quantity with the same dimension) that the value $\epsilon = 0$ has a physical meaning, distinguishing the sign of the work done on the system by the external forces. We found that the corresponding β leads to a possible definition of a "temperature". The problem we have in many experiments for which $P(t)$ does not take negative values, is related to

the fact that equation (1) remains valid if an arbitrary constant is added to both P and D. A possible choice to analyze turbulent data would be to determine the mean flow and to subtract from $P(t)$ the power necessary to maintain the mean flow. This will be difficult to compute in most experimental configurations but could be easily tried on direct numerical simulations. A simpler possibility would be to use the above remark and to define arbitrarily a zero of $P(t)$ with the hope that the scaling of β with respect to $\langle E \rangle$ and the number of degrees of freedom does not crucially depend on the choice of the origin. This could be checked in many cases and clearly deserves more experimental or numerical studies.

We acknowledge useful discussions with F. Bonetto, E. Cohen, B. Derrida, U. Frisch, J. Kurchan and E. Tirapegui .

References

1. S. Ciliberto, S. Douady, S. Fauve, Europhys. Lett. **15**, 23 (1991).
2. R. Labbé, J.F. Pinton, S. Fauve, J. Phys. II France **6**, 1099 (1996).
3. S. Aumaitre, S. Fauve, J. Chim. Phys. **96**, 1038 (1999).
4. D.J. Evans, E.G.D. Cohen, G.P. Moriss, Phys. Rev. Lett. **71**, 2401 (1993).
5. G. Gallavotti, E.G.D. Cohen, Phys. Rev. Lett. **74**, 2694 (1995).
6. J. Kurchan, J. Phys. A **31**, 3719 (1998).
7. E.B. Gledzer, Sov. Phys. Dokl. **18**, 216 (1973).
8. V. Desnyansky, E. Novikov, Prikl. Mat. Mekh. **38**, 507 (1974).
9. M. Yamada, K. Ohkitani, J. Phys. Soc. Jpn **56**, 4210 (1987).
10. M.H. Jensen, G. Paladin, A. Vulpiani, Phys. Rev. A **43**, 798 (1991).
11. D. Pisarenko, L. Biferale, D. Courvoisier, U. Frisch, M. Vergassola, Phys. Fluids A **5**, 2533 (1993).
12. J.-F. Pinton, R. Labbé, P. Holdsworth, Phys. Rev. E **60**, 2454 (1999).
13. A. Pumir, Phys. Fluids **8**, 3112 (1996).
14. S. Warr, J.M. Huntley, G.T.H. Jacques, Phys. Rev. E **52**, 5583 (1995).
15. E. Falcon, S. Fauve, C. Laroche, Eur. Phys. J. B **9**, 183 (1999).
16. E. Falcon, R. Wunenburger, P. Evesque, S. Fauve, C. Chabot, Y. Garrabos, D. Beysens, Phys. Rev. Lett. **83**, 440 (1999).
17. S. McNamara, S. Luding, Phys. Rev. E **58**, 813 (1998), and references therein.
18. W. Feller, *An introduction to probability theory and its applications*, 2nd edn. (John Wiley and Sons, New York, 1966), Vol. II, pp. 47–49.
19. S. McNamara, W. Young, Phys. Rev. E **53**, 5089 (1996).
20. This is also true for turbulence. The PDF of the injected energy depends on the way the fluid is driven.
21. R. Burridge, L. Knopoff, Bull. Seismol. Soc. Am. **57**, 341 (1967).
22. J.M. Carlson, J.S. Langer, Phys. Rev. Lett. **62**, 2632 (1989).
23. M. de Sousa Vieira, Phys. Rev. A **46**, 6288 (1992).
24. G. Gallavotti, Chaos **8**, 384 (1998).
25. R.S. Ellis, *Entropy, large deviations and statistical mechanics* (Springer Verlag, New York, 1985).
26. Y. Oono, Prog. Theor. Phys. **99**, 165 (1989).
27. G. Gallavotti, Physica A **263**, 39 (1999).
28. G. Gallavotti, Phys. Lett. A **223**, 91 (1996).
29. It has been shown on an example of time reversible system, that taking into account only one part of the system may lead to a wrong determination of β, F. Bonetto, N.I. Chernov, J.L. Lebowitz, Chaos **8**, 823 (1998).
30. S. Ciliberto, C. Laroche, J. Phys. IV France **8**, Pr6-215 (1998).
31. S. Aumaître, Ph.D. thesis, ENS-Lyon, 1999.